

# 1 Regionalization of Europe based on a $K$ -Means Cluster Analysis of the 2 climate change of Temperatures and Precipitation

3 M. J. Carvalho<sup>a</sup>, P. Melo-Gonçalves<sup>a</sup>, J. C. Teixeira<sup>a</sup>, A. Rocha<sup>a</sup>

4 <sup>a</sup>*Department of Physics & CESAM, University of Aveiro, Aveiro, Portugal*

---

## 5 **Abstract**

In order to study climate change on a regional scale using Earth System Models, it is useful to partition the spatial domain into regions according to their climate changes. The aim of this work is to divide the European domain into regions of similar projected climate changes using a simulation of daily total precipitation, minimum and maximum temperatures for the recent-past (1986 – 2005) and long-term future (2081 – 2100) provided by the Coupled Model Intercomparison Project (CMIP5). The difference between the long-term future and recent-past daily climatologies of these three variables is determined. Aiming to objectively identify the grid points with coherent climate changes, a  $K$ -Mean Cluster Analysis is applied to these differences. This method is performed for each variable independently (univariate version) and for the aggregation of the three variables (multivariate version). A mathematical approach to determine the optimal number of clusters is pursued. However, due to the method characteristics, a sensitivity test to the number of clusters is performed by analysing the consistency of the results. This is a novel method, allowing for the determination of regions based on the climate change of multiple variables. Results from this method are in accordance with results found in the literature, showing overall similar regions of changes.

6 *Keywords:* Climate Change, Surface Temperatures,  $K$ -Means Clustering, Precipitation, Europe

---

## 7 **1. Introduction**

8 Climate change studies are usually carried out either globally or regionally. Either way, they usu-  
9 ally focus on areas with different climate characteristics and large variability. In Europe, temporal  
10 variability of daily surface climate variables (such as minimum and maximum temperatures and

11 precipitation) has high spatial gradients. Therefore, statistics of the temporal behaviour of a par-  
12 ticular variable or its derived quantities over the target domain must be estimated taking into  
13 account these spatial gradients. Some statistics can be displayed over a map; however there are  
14 statistics, such as Probability Density Functions at each grid point of the domain, that are impos-  
15 sible to be displayed in a map. Because of this, it is mandatory to reduce the number of degrees of  
16 freedom which, in this case, consists of a reduction of the time series representative of the domain.  
17 This, together with the large amount of data, adds up to the need to define regions to be analysed  
18 using either grid point as a representation of the region or the average behaviour of the grid points.

19  
20 In an attempt to divide the overland areas of the globe into a manageable number of regions,  
21 each with simple shape and representing a different climatic regime, several authors (such as  
22 [Sillmann et al. \(2013, 2014\)](#)) have followed the approach of [Giorgi and Francisco \(2000\)](#). When  
23 studying the uncertainty in regional climate change prediction using ensemble simulations from  
24 a coupled Atmosphere-Ocean Global Climate Model (AOGCM), they proposed a division of the  
25 domain, creating rectangle-like overland areas, admitting, however, that this was a subjective ap-  
26 proach to the issue. On a regional scale, the simple use of geographic markers has been extensively  
27 used in order to define regions. For example, in their study of European heat waves in present-day  
28 and future climates, [Lau and Nath \(2014\)](#) simply divided the domain into three regions: Russia,  
29 eastern Europe and western Europe. Much like this, when studying record high maximum and  
30 low minimum temperatures, [Meehl et al. \(2009\)](#) used the 100°W meridian to divide the United  
31 States of America into eastern and western USA. [Fischer and Schär \(2009\)](#) simply use the Iberian  
32 Peninsula, Scandinavia and France as key regions when studying the PRUDENCE regional cli-  
33 mate model scenarios for temperature and the driving processes in temperature extremes while  
34 [Wójcik \(2014\)](#) divides Poland taking into account some orographic characteristic in order to study  
35 the reliability of CMIP5 simulations in reproducing atmospheric circulation. An upgrade to this  
36 methodology is the approach of [Fischer et al. \(2014\)](#) who segregate grid points based on their alti-  
37 tude, in order to study projected changes in precipitation intensity and frequency in Switzerland.

38

39 Due to the subjectivity of the regionalization methodologies described above, several authors have  
40 pursued a more objective approach. For example, [Richman and Lamb \(1985, 1987\)](#) used Principal  
41 Component Analysis (PCA) in order to study the spatial distribution of three- and seven-day  
42 rainfall events for the USA and Canada, respectively. In a later work, [White et al. \(1991\)](#) applied  
43 Rotation Principal Analysis to monthly precipitation in Pennsylvania using different rotation al-  
44 gorithms in order to assess the sensitivity of the regionalization result to rotation. They found  
45 that the resulting regions varied widely with the use of different rotation algorithms.

46

47 In addition to having been used to identify Weather Types (or Weather Regimes) by [Santos et al.](#)  
48 [\(2005\)](#), Cluster Analysis has also been used to define climatic regions. [DeGaetano and Shulman](#)  
49 [\(1990\)](#) applied a flexible clustering technique to the first three principal components of several  
50 climatological variables in order to identify regions of coherent plant hardiness. Much like this,  
51 [Fovell and Fovell \(1993\)](#) used *K*-Means Cluster Analysis in order to identify climatic zones of the  
52 Conterminous United States based on both temperature and precipitation.

53

54 However objective these studies may be, they regionalize the domain using observed (or mod-  
55 eled) data for a given period and therefore obtain regions of coherent climate. In a changing  
56 climate, the main interest becomes knowing the regions of coherent changes, instead of the defini-  
57 tion of regions with the same climate characteristics, since they can change in time. The main goal  
58 of this work was to identify regions with consistent climate changes in precipitation and surface  
59 minimum and maximum temperature seasonal cycles in Europe. This is a novel method, allowing  
60 for the determination of regions based on the climate change of multiple variables.

## 61 **2. Method and Data**

62 The data used was provided by the Coupled Model Intercomparison Project Phase 5 (CMIP5),  
63 simulated by the MPI-ESM-LR model with the r1i1p1 initialization, with a horizontal resolution of  
64 1.9° horizontal resolution ([Giorgetta et al., 2013](#)). As a representation of the recent-past climate,  
65 the last 20 years (1986 – 2005) of the historical experiment which runs from 1850 to 2005 were used.

66 The future climate used was simulated by using the 8.5 Representative Concentration Pathway  
67 (RCP8.5) which stabilizes radiative forcing at  $8.5 \text{ W} \cdot \text{m}^{-2}$  in the year 2100 without exceeding that  
68 value (Riahi et al., 2011). From the future climate experiment, which runs from 2006 to 2100,  
69 only the long-term future (from 2081 to 2100) was used in this work, since changes for this period  
70 relative to the recent-past are expected to be greater than those found for both the near-term  
71 (2016 – 2035) and mid-term (2046 – 2065) periods. The variables used were the daily minimum  
72 and maximum near-surface air temperatures as well as total daily precipitation, which includes  
73 both liquid and solid phases from all types of clouds (both large scale and convective). The simu-  
74 lations are available for the entire globe. However, this study focused on a domain containing only  
75 Europe:  $25^\circ\text{N} - 70^\circ\text{N}, 45^\circ\text{W} - 65^\circ\text{E}$ . This domain is presented in Figure 1 where the model grid  
76 points corresponding to the aforementioned resolution are also plotted.

77  
78 Taking each of the two climates – recent-past and long-term future – daily climatologies of each of  
79 the variables were determined, for each of the domain grid points, using a 15 day-running window  
80 as a low frequency filter. Taking each grid point, the difference between the recent-past and long-  
81 term future climatologies were determined, creating a measure of the changes in the seasonal cycle.

82  
83 The challenge was then identifying grid points where the changes in the seasonal cycle of the  
84 variables are similar. To the difference fields, the  $K$ -Means Cluster Analysis was applied. This is  
85 a non-hierarchical clustering method which starts by computing the centroids for each cluster and  
86 then calculates the distances between the current data vector and each of the centroids, assigning  
87 the vector to the cluster whose centroid is closest to it. Since this is a dynamic method, meaning  
88 that vectors can change cluster after being assigned to it, this process is repeated until all vectors  
89 are assigned a cluster and their members are closest to the centroid than to the mean of other  
90 clusters (Wilks, 2011). The mathematical condition for the cluster  $C_k$  and the  $k$  centroids  $\mu_k$  can  
91 be expressed as Equation 1.

$$\text{Minimize } \sum_{k=1}^K \sum_{x_n \in C_k} \|x_n - \mu_k\|^2 \quad \text{with respect to } C_k, \mu_k \quad (1)$$

92 It is important to note that, unlike when applied to determine weather types, the *K*-Means Clus-  
93 tering is done in space and not time, resulting in each grid point (instead of a time step) being  
94 assigned to a cluster.

95

96 The described methodology was applied to the climatology differences of each of the three vari-  
97 ables independently (univariate version) and using the daily climatology differences of a synthetic  
98 joint variable composed by concatenating the temporal-varying spatial fields of the three variables  
99 (multivariate version). Since the goal is to determine one set of regions on which to base the anal-  
100 ysis, the univariate version is only used to, once more, analyse the consistency of the multivariate  
101 results and ultimately validate them, since this is a novel statistical approach.

102

103 In order to determine the number of clusters, the Gap Statistics was used as described by [Pham](#)  
104 [et al. \(2005\)](#). However, since this is a blind statistic, the sensitivity to the number of clusters was  
105 estimated by computing the *K*-Means for different *k*'s, which allowed for the verification of the  
106 results' consistency.

107

108 Lastly, the statistical significance of the differences between the regional averaged long-term future  
109 and recent-past daily climatologies for each variable was estimated using the non-parametric Rank-  
110 sum test ([Mann and Whitney, 1947](#)). This test was chosen due to its resistance to wild data or  
111 outliers which could otherwise contaminate the results by providing false negatives ([Wilks, 2011](#)).  
112 Furthermore, since it is a non-parametric test, it does not require data with a normal probability  
113 distribution.

### 114 **3. Results and Discussion**

115 Due to the chosen clustering method, the number of clusters, *k*, must be chosen a priori. Using  
116 the Gap Statistics as described in Section 2, it was determined that *k* = 6 was the optimal choice.  
117 As mentioned before, since this is a purely mathematical method, the clustering analysis was also  
118 performed with *k* = 3, 10 and 13. For each *k*, the method was applied to each of the variables

119 individually, followed by the multivariate version. For the sake of conciseness, and since the  
120 univariate version serves as a validation of coherence, only the results of the multivariate cluster  
121 analysis will be presented.

### 122 *3.1. Regionalization*

123 When applying the clustering algorithm to each of the variables using  $k = 3$  (results not shown),  
124 the domain is divided into three regions which are similar for maximum and minimum tempera-  
125 tures, with the exception of the Mediterranean region which is grouped together with the Atlantic  
126 region for minimum temperature and with northern Europe for maximum temperature. Precipita-  
127 tion regions show a clear division of Europe into two along the  $55^\circ\text{N}$  latitude, with the third region  
128 located northwest of Iceland being considerably smaller. Results obtained by the multivariate ver-  
129 sion, shown in Figure 2a), are consistent with those obtained by the univariate one. There is a  
130 region south of  $40/50^\circ\text{N}$  latitude, which includes north Africa, the Mediterranean, Italy, Greece  
131 and most of the Iberian Peninsula. The second (middle) region goes from the  $40/50^\circ\text{N}$  latitude  
132 up to  $60^\circ\text{N}$  overland, and encroaches up to the upper boundary of the domain over the Atlantic  
133 ocean. The third regions encloses two subregions: northern Europe (north of  $60^\circ\text{N}$ ) and Greenland.

134  
135 When the number of clusters is increased, there are more regions to which each point can be at-  
136 tributed and therefore the regions obtained will provide a more detailed definition of the changes.  
137 As for  $k = 3$ , the  $k = 6$  regions obtained for maximum and minimum temperatures are similar  
138 and differ from the precipitation ones especially over the Atlantic ocean, in the western most part  
139 of the domain. In this area, there is a larger number of regions for precipitation while there is  
140 more differentiation over land when temperature is used. The regions based on the precipitation  
141 changes follow the approximate layering described for the multivariate  $k = 3$  regionalization for  
142 the overland area while, for the western side of the  $20^\circ\text{W}$  meridian, there is an increased number  
143 of regions from three to four. Results obtained by the multivariate version, shown in Figure 2b),  
144 approximately follow the temperature ones; there is a small region over Greenland and a larger  
145 region over the northern part of the Atlantic. The southern region of the Atlantic ocean belongs  
146 to a distinct region which extends into the Mediterranean and includes countries such as Por-

147 tugal, southern Spain, western France, and Italy). Overland points in Africa are grouped into  
148 another region, while the remaining parts of Europe are divided once more approximately along  
149 the 55/60°N parallel. The fact that so many overland points belong to the southern-Atlantic and  
150 Mediterranean region is most likely due to the combined effect of the model's coastline and its low  
151 resolution.

152  
153 The results for  $k = 3$  results show that there is a latitudinal layering of the changes affecting pre-  
154 cipitation as well as maximum and minimum temperatures in Europe. These results are consistent  
155 with the work of [Field et al. \(2014\)](#) who have shown that there is a clear latitudinal differentiation  
156 of climate change of precipitation and temperatures, as well as extreme events such as dry spells  
157 and heat waves. Also, there is a distinctive area of changes in central Europe which, in this study,  
158 appears in the  $k = 6$  regionalization.

159  
160 When applying  $k = 10$ , the number of regions is higher over the Atlantic for precipitation and  
161 over land for the temperatures, even though more balanced than what was found for a lower  $k$ .  
162 Also, in the univariate versions of the clustering, the regions become less organized and layered  
163 when compared to what happened for a lower  $k$ . However, the multivariate regionalization shown  
164 in [Figure 2c](#)) retains the horizontal layering format, even though presenting differences between  
165 overland and over-ocean areas. The north African region, obtained for  $k = 3$  and 6, become di-  
166 vided into two distinct regions: one between the 30°N and 40°N parallels in the overland points,  
167 and another below the southern parallel. Once more Europe is divided into three belt regions:  
168 the first between the 40°N and 50°N parallels, the second up to the 60°N and the third, north of  
169 that. It is noteworthy that some grid points in the southern Iberian Peninsula are attributed to  
170 the same region as north Africa. However, this should be considered carefully since the connection  
171 between the two parts of the region, as well as the Iberian part of the region itself, is cell-thin.  
172 Over the ocean, one of the regions includes the entire Atlantic below 40°N, encroaching into the  
173 Mediterranean (similar with a region found for  $k = 6$ ). Above that, there is another region which  
174 is bordered above and to the west by a different one. As seen for  $k = 6$ , there is also another

175 distinct region over Greenland.

176

177 When moving to  $k = 13$ , the increase in regions is still distributed the same way (more regions  
178 over the ocean for precipitation and more regions overland for temperature). However, and as can  
179 be seen in Figure 2d) there are several cell-thin regions which leads to the belief that the number  
180 of clusters is too high for the spatial resolution of this model.

181

182 From the comparison of results obtained from different  $k$ 's in the  $K$ -Means algorithm, it can  
183 be concluded that  $k = 6$  is, as predicted by the Gap Statistics, the best choice. It could be argued  
184 that applying  $k = 10$  to the multivariate version of the clustering method yields equally good re-  
185 sults with the added value of a more localized regionalization. However, when using the univariate  
186 version, there are several cases of cell-thin regions suggesting that this number of clusters is too  
187 high for the resolution in use.

### 188 *3.2. Validation of the $k$ regions*

189 Since both the Gap Statistics and the analysis of the results for different number of clusters points  
190 to six being the optimum  $k$ , it is worth looking into the differences in climatologies of the variables  
191 for each of the different regions. These differences can, not only show the differences between  
192 regions, but also serve as an objective characterization of the regions in terms of their climate  
193 change patterns in the long-term future.

194

195 Since the regions were defined based on climate change in the seasonal cycle of precipitation, max-  
196 imum and minimum temperature, it is worth comparing the Probability Distribution Functions  
197 (PDFs) of two climates (recent-past and long-term future) of each region (Figure 3d) – i)). The  
198 Rank-Sum statistical test (see Section 2) was applied to the PDFs of the two climates. The only  
199 regions for which the long-term future climate is considered to be different is R1 (with a confidence  
200 level of 95%) and R4 (confidence level 90%) and only for precipitation. The remaining PDFs can-  
201 not be considered significantly different. However, and since it was the daily climatology difference  
202 that was used to define the clusters, that was also tested using the Rank-Sum test. When testing

203 the region-averaged daily climatologies of the long-term future against those of the recent-past, the  
204 results show that, for all six regions, the long-term future daily climatology is distinct from the  
205 recent-past one at a confidence level of 99%. These results point to an interesting development.  
206 While there is, on average, no significant climate change detection in the PDFs of the variables,  
207 for all the regions, that change is present and statistically significant in the climatologies, showing  
208 that, while detecting seasonal changes, those might not be evident in the original PDFs.

209

210 On the left column of Figure 3, the mean regional seasonal climatological differences (deviations of  
211 the long-term future climatology from the recent-past climatology) for each variable can be seen,  
212 for the six regions. For all three variables, it is evident that each region presents different climato-  
213 logical changes, which vary throughout the seasons in distinct ways. That said, it can be seen that  
214 the climatological differences are always positive for both minimum and maximum temperatures  
215 (top two plots), pointing to a warming of all regions, albeit of different magnitude. Overall, the  
216 seasonal differences between the recent-past and long-term future are statistically significant at  
217 the 95% confidence level for temperatures and precipitation, for all regions. The exceptions are  
218 R2 and R6 in spring and R1 and R6 for autumn (marked with the asterisks).

219

220 The regions showing largest climatological differences for both temperatures are R1 (north-Atlantic),  
221 R3 (northern Africa) and R6 (Central and eastern Europe) followed by R5 (Greenland). The largest  
222 differences found are for R3, with minimum temperature changes reaching an 8 °C increase (6 °C  
223 in maximum temperature) in the future during winter, and a 5 °C increase in both temperatures  
224 throughout the remaining seasons. On the other hand, R2 (northern Europe) and R4 (southern  
225 part of the Atlantic extending to the Mediterranean and IP) show the lowest magnitude of changes,  
226 ranging from  $\sim 2.5^{\circ}\text{C}$  for the earlier and  $\sim 3.5^{\circ}\text{C}$  for the later. These results point to a stronger  
227 warming in areas where temperatures tend to be more extreme, such as north Africa and central  
228 Europe which are warmer and Greenland where temperatures tend to be lower.

229

230 When compared to temperature, precipitation changes (lower plot) show a different scenario,

231 with a less organized seasonal pattern, which would be expected due to the fact that precipitation  
 232 (unlike temperature) is neither continuous in time or space. The regions which show higher and  
 233 therefore significant changes throughout the seasons are R3, R4 and R5. In magnitude, the season  
 234 showing largest changes is autumn with a decrease of  $\sim 0.7$  mm (R4 + R6) and increase of 1.5 mm  
 235 (R2 + R3 + R5). R4, or the southern Atlantic and Mediterranean region shows a systematic  
 236 and significant decrease of precipitation through the seasons while regions such as northern Africa  
 237 (R3) and Europe (R2) and Greenland (R6) show increase in precipitation. Central Europe shows  
 238 a redistribution of the rainfall patterns through the seasons, with its decrease in precipitation is  
 239 mainly due to the summer. As for temperature, it is clear that the largest changes are projected  
 240 for the most arid area of the domain (north Africa), as well as snow prone regions such as north  
 241 Atlantic and Greenland.

242

243

Table 1: Cross-test of the regions to determine if the daily climatologies of each of the variables are significantly different for each region. Checks represent pairs of regions which have shown to be distinct from each other for all three variables, at the 95% confidence level. The remaining pairs are considered to have the same distributions for the mentioned variable. Dark gray cells show pairs of regions for which the precipitation distributions are considered to be different, but only at the 90% confidence level.

	R1	R2	R3	R4	R5	R6
R1		✓	tasmax	✓	tasmin	pr
R2			✓	✓	pr	✓
R3				✓	pr	✓
R4					✓	✓
R5						tasmax
R6						

244 In order to verify if the regions are significantly different from each other, the Rank-sum statistical  
 245 test was applied to each pair of regions, at the 95% confidence level (Table 1). The only region

246 which is considered to be significantly different from all others at a 95% confidence level for all  
247 three variables under study is R4. However, if the confidence level is lowered to 90%, R2 also passes  
248 the test for all variables and is therefore concluded to be distinct from the other regions. Even  
249 though the distribution of one of the variables is not significantly different for some pairs of regions  
250 (as happens with R1 and R3 and R5 and R6 for maximum temperature, R1 and R5 for minimum  
251 temperature and R3 and R5 for precipitation), it is worth considering these regions as having  
252 different characteristics since the clustering is performed on several features (i.e. variables) rather  
253 than just one. This outcome shows a shortfall of this methodology which is, however, overcome  
254 by the fact that the method produces one set of regions based on the climate change of a group of  
255 variables.

#### 256 4. Concluding Remarks

257 This work aims to develop a novel approach to the regionalization of a domain, in this case Europe,  
258 based on the climate change of a range of variables. The focus was on the long-term changes in  
259 precipitation, maximum and minimum temperatures. This was achieved by applying a  $K$ -Means  
260 clustering analysis to the daily climatological difference for each of the variables independently  
261 (univariate – not shown) and, most importantly, using each of the variables as a feature (multi-  
262 variate version). The result is a map in which each grid point is associated to a cluster (region).

263  
264 Results show that the multivariate version is congruent with the univariate version, although cre-  
265 ating new and more intricate features in the regions. For the optimum determined  $k$  (six), there  
266 is a clear latitudinal layering of the regions, which is then overrun by the inland-ocean differences.  
267 The Atlantic Ocean area is divided into northern and southern part, with the later extending over  
268 the Iberian Peninsula and the Mediterranean. Greenland, north Africa, Central to eastern and  
269 northern Europe comprise the other four regions.

270  
271 When analysing the seasonally averaged climatology differences for each region, it becomes clear  
272 that these regions have, in fact, different characteristics concerning precipitation, maximum and

273 minimum temperature projected changes, even though these are not statistically significant for  
274 every variable when region pairs are compared.

275

276 It is noteworthy that the maximum and minimum temperature changes projected for the long-term  
277 are positive and statistically significant in every region, pointing to a clear warming of Europe, for  
278 every season. Precipitation changes show a more complex outlook, with the Mediterranean and  
279 southern Atlantic showing a systematic and significant decrease in precipitation and regions such  
280 as northern Africa and Europe and Greenland showing increase.

281

282 The sensitivity of the results to the number of regions was tested by performing the same method-  
283 ology for  $k = 3, 6, 10, 13$ . Results show that, when increasing the number of clusters considered  
284 there is increased detail in the spatial features obtained. However, due to the rather coarse reso-  
285 lution of the data, when  $k = 10, 13$ , single grid points of a region engulfed by other regions start  
286 to appear. These features may not be geographical and therefore, the number of clusters needs  
287 adaptation for different resolutions.

288

289 Even though the seasonal climate change detected is not evident on the Probability Distribu-  
290 tion Functions of the original variables and that some regions were found to not be significantly  
291 different from each other concerning the changes of a variable, this methodology presents a novel  
292 way to approach the subject of identifying regions of coherent climate change. Furthermore, it  
293 creates the possibility to determine areas based on several variables, rather than just one.

## 294 **5. Acknowledgments**

295 This study was supported by FEDER funds through the Programa Operacional Factores de Com-  
296 petitividade – COMPETE and by Portuguese national funds through FCT – Fundação para a  
297 Ciência e a Tecnologia, within the framework of the following projects: CLIPE Project Reference  
298 PTDC/AAC-CLI/111733/2009; CLICURB EXCL/AAG-MAA/0383/2012. We acknowledge the  
299 World Climate Research Programme’s Working Group on Coupled Modelling, which is responsible

300 for CMIP, and we thank the Max Planck Institute for Meteorology for producing and making  
301 available their model output as described in Section 2. For CMIP the U.S. Department of En-  
302 ergy’s Program for Climate Model Diagnosis and Intercomparison provides coordinating support  
303 and led development of software infrastructure in partnership with the Global Organization for  
304 Earth System Science Portals

## 305 6. References

- 306 DeGaetano, A. T., Shulman, M. D., 1990. A climatic classification of plant hardiness in the United  
307 States and Canada. *Agricultural and forest meteorology* 51 (3), 333–351.
- 308 Field, C. B., Barros, V. R., Mach, K., Mastrandrea, M., 2014. Climate change 2014: impacts,  
309 adaptation, and vulnerability. Contribution of Working Group II to the Fifth Assessment Report  
310 of the Intergovernmental Panel on Climate Change.
- 311 Fischer, A., Keller, D., Liniger, M., Rajczak, J., Schär, C., Appenzeller, C., 2014. Projected changes  
312 in precipitation intensity and frequency in Switzerland: a multi-model perspective. *International*  
313 *Journal of Climatology*.
- 314 Fischer, E. M., Schär, C., 2009. Future changes in daily summer temperature variability: driving  
315 processes and role for temperature extremes. *Climate Dynamics* 33 (7-8), 917–935.
- 316 Fovell, R. G., Fovell, M.-Y. C., 1993. Climate zones of the conterminous United States defined  
317 using cluster analysis. *Journal of Climate* 6 (11), 2103–2135.
- 318 Giorgetta, M. A., Jungclaus, J., Reick, C. H., Legutke, S., Bader, J., Böttinger, M., Brovkin, V.,  
319 Crueger, T., Esch, M., Fieg, K., et al., 2013. Climate and carbon cycle changes from 1850 to  
320 2100 in MPI-ESM simulations for the Coupled Model Intercomparison Project phase 5. *Journal*  
321 *of Advances in Modeling Earth Systems* 5 (3), 572–597.
- 322 Giorgi, F., Francisco, R., 2000. Uncertainties in regional climate change prediction: a regional  
323 analysis of ensemble simulations with the HADCM2 coupled AOGCM. *Climate Dynamics* 16 (2-  
324 3), 169–182.

- 325 Lau, N.-C., Nath, M. J., 2014. Model simulation and projection of European heat waves in present-  
326 day and future climates. *Journal of Climate* 27 (10), 3713–3730.
- 327 Mann, H. B., Whitney, D. R., 1947. On a test of whether one of two random variables is stochas-  
328 tically larger than the other. *The annals of mathematical statistics*, 50–60.
- 329 Meehl, G. A., Tebaldi, C., Walton, G., Easterling, D., McDaniel, L., 2009. Relative increase of  
330 record high maximum temperatures compared to record low minimum temperatures in the US.  
331 *Geophysical Research Letters* 36 (23).
- 332 Pham, D. T., Dimov, S. S., Nguyen, C., 2005. Selection of K in K-means clustering. *Proceedings*  
333 *of the Institution of Mechanical Engineers, Part C: Journal of Mechanical Engineering Science*  
334 219 (1), 103–119.
- 335 Riahi, K., Rao, S., Krey, V., Cho, C., Chirkov, V., Fischer, G., Kindermann, G., Nakicenovic, N.,  
336 Rafaj, P., 2011. RCP 8.5 – A scenario of comparatively high greenhouse gas emissions. *Climatic*  
337 *Change* 109 (1-2), 33–57.
- 338 Richman, M. B., Lamb, P. J., 1985. Climatic pattern analysis of three-and seven-day summer  
339 rainfall in the central United States: Some methodological considerations and a regionalization.  
340 *Journal of Climate and Applied Meteorology* 24 (12), 1325–1343.
- 341 Richman, M. B., Lamb, P. J., 1987. Pattern analysis of growing season precipitation in southern  
342 Canada. *Atmosphere-Ocean* 25 (2), 137–158.
- 343 Santos, J., Corte-Real, J., Leite, S., 2005. Weather regimes and their connection to the winter  
344 rainfall in Portugal. *International Journal of Climatology* 25 (1), 33–50.
- 345 Sillmann, J., Donat, M. G., Fyfe, J. C., Zwiers, F. W., 2014. Observed and simulated temperature  
346 extremes during the recent warming hiatus. *Environmental Research Letters* 9 (6), 064023.
- 347 Sillmann, J., Kharin, V., Zhang, X., Zwiers, F., Bronaugh, D., 2013. Climate extremes indices in  
348 the CMIP5 multimodel ensemble: Part 1. Model evaluation in the present climate. *Journal of*  
349 *Geophysical Research: Atmospheres* 118 (4), 1716–1733.

- 350 White, D., Richman, M., Yarnal, B., 1991. Climate regionalization and rotation of principal com-  
351 ponents. *International Journal of Climatology* 11 (1), 1–25.
- 352 Wilks, D. S., 2011. *Statistical methods in the atmospheric sciences*. Vol. 100. Academic press.
- 353 Wójcik, R., 2014. Reliability of CMIP5 GCM simulations in reproducing atmospheric circulation  
354 over Europe and the North Atlantic: a statistical downscaling perspective. *International Journal*  
355 *of Climatology*.

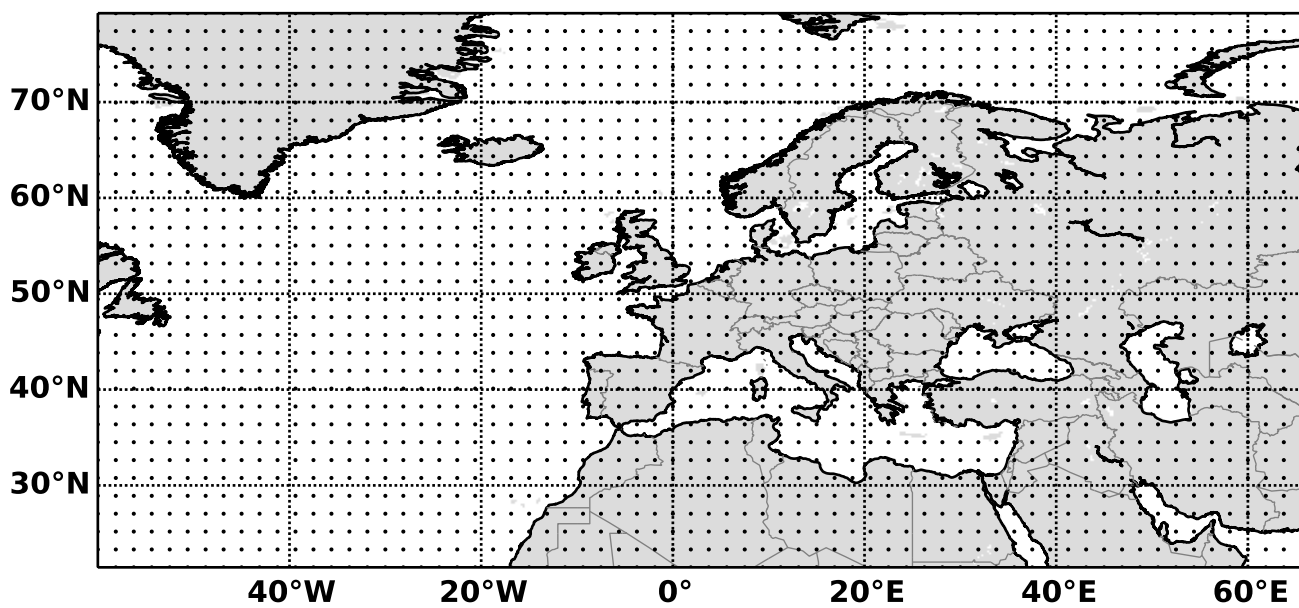


Figure 1: Study domain to which the MPI-ESM-LR Earth System Model data was cut and model grid points ( $1.9^\circ$  horizontal resolution).

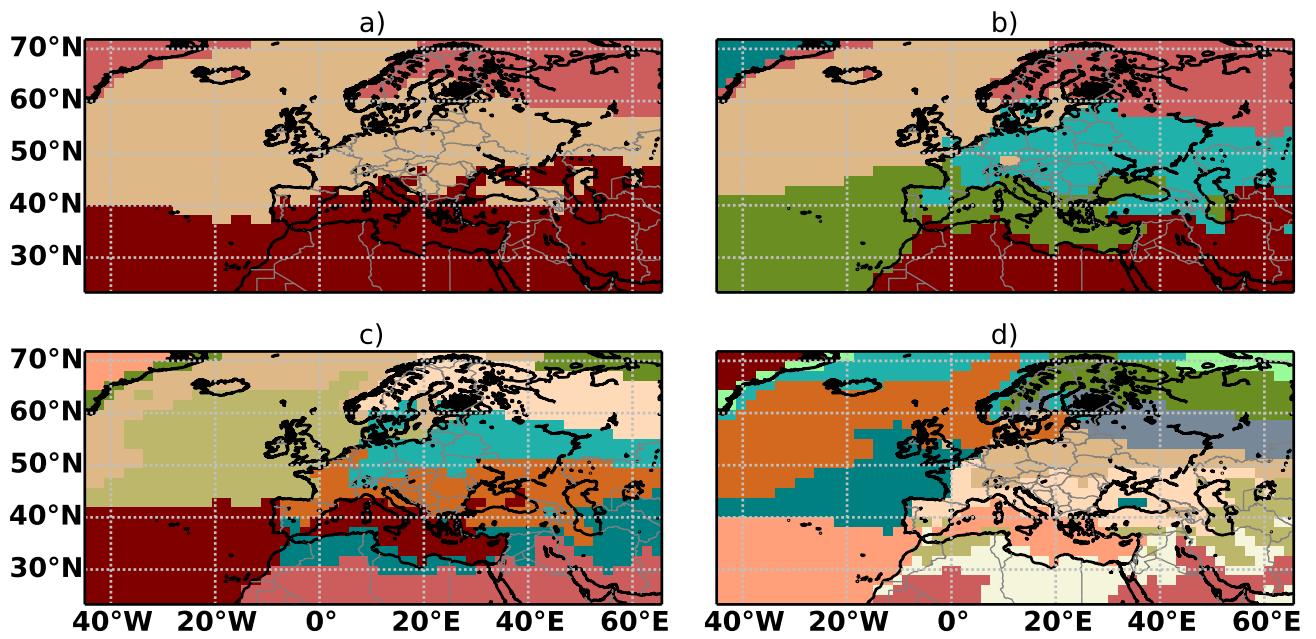


Figure 2: Regions in Europe as determined using *K*-Means Clustering Analysis applied to the climatology difference between the recent-past (1986 – 2005) and long-term future (2081 – 2100) using a)  $k = 3$ , b)  $k = 6$ , c)  $k = 10$  and d)  $k = 13$ . Note that the colors are not correspondent to each other from panel to panel and that they only serving only to allow better differentiation between regions inside each panel.

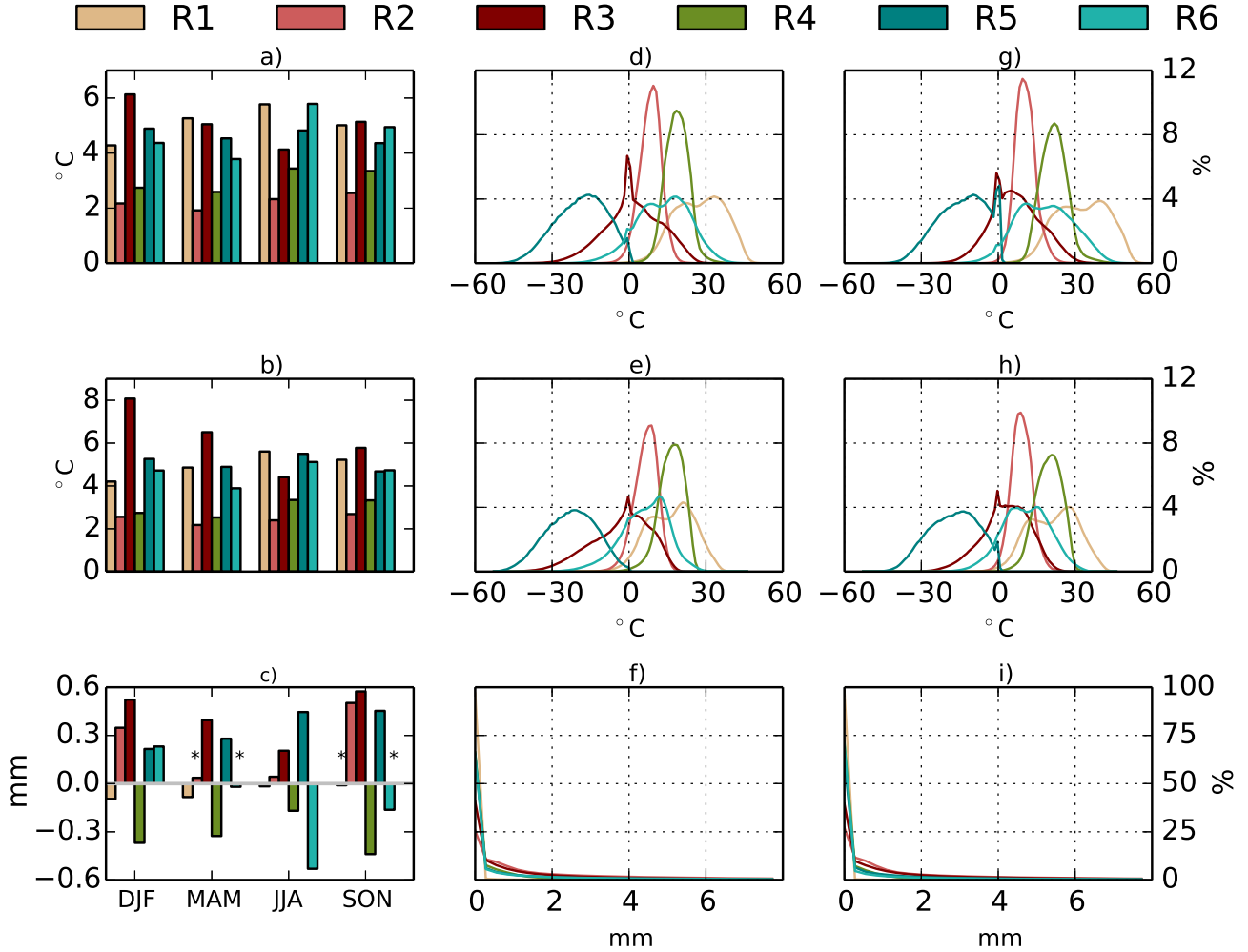


Figure 3: The seasonal average of the daily climatology difference between the recent-past (1986 – 2005) and long-term future (2081 – 2100) for a) maximum temperature, b) minimum temperature and c) daily total precipitation, for each of the six regions obtained using the multivariate *K*-Means clustering analysis is on the left column. Asterisks mark where the mean seasonal climatology difference is not statistically significant at the 95% confidence level. The middle and right column represent the Probability Distribution Functions of d) maximum temperature, e) minimum temperature and f) precipitation for the 1986 – 2005 and 2081 – 2100 periods respectively. These regions are color-coherent with the regions in Figure 2.b).